Molecular Biology of the Cell
Vol. 19, 1241–1251, March 2008

RNA Interference in J774 Macrophages Reveals a Role for Coronin 1 in Mycobacterial Trafficking but Not in Actin-dependent Processes

Rajesh Jayachandran,* John Gatfield,* Jan Massner, Imke Albrecht, Bettina Zanolari, and Jean Pieters

Biozentrum, University of Basel, 4056 Basel, Switzerland

Submitted July 9, 2007; Revised November 20, 2007; Accepted December 14, 2007
Monitoring Editor: Sandra Schmid

Macrophages are crucial for innate immunity, apoptosis, and tissue remodeling, processes that rely on the capacity of macrophages to internalize and process cargo through phagocytosis. Coronin 1, a member of the WD repeat protein family of coronins specifically expressed in leukocytes, was originally identified as a molecule that is recruited to mycobacterial phagosomes and prevents the delivery of mycobacteria to lysosomes, allowing these to survive within phagosomes. However, a role for coronin 1 in mycobacterial pathogenesis has been disputed in favor for its role in mediating phagocytosis and cell motility. In this study, a role for coronin 1 in actin-mediated cellular processes was addressed using RNA interference in the murine macrophage cell line J774. It is shown that the absence of coronin 1 in J774 macrophages expressing small interfering RNA constructs specific for coronin 1 does not affect phagocytosis, macropinocytosis, cell locomotion, or regulation of NADPH oxidase activity. However, in coronin 1-negative J774 cells, internalized mycobacteria were rapidly transferred to lysosomes and killed. Therefore, these results show that in J774 cells coronin 1 has a specific role in modulating phagosome–lysosome transport upon mycobacterial infection and that it is dispensable for most F-actin–mediated cytoskeletal rearrangements.

INTRODUCTION

The coronin protein family consists of a series of highly conserved proteins that are found in all eukaryotic species (Okumura *et al*., 1998). Coronin was originally isolated as an actin/myosin-interacting protein from *Dictyostelium discoideum* (de Hostos *et al*., 1991). In *Dictyostelium*, coronin is involved in phagocytosis, macropinocytosis, cell locomotion, and cytokinesis (de Hostos *et al*., 1993; Gerisch *et al*., 1993). In yeast, there is a single coronin homologue (*Crn1*) that interacts in vitro with the actin-related protein 2/3 (Arp2/3) complex, and it has been proposed to regulate the formation of actin filamentous networks (Humphries *et al*., 2002). In mammalian cells, up to seven coronin isoforms have been identified of which coronins 2 and 3 are ubiquitously expressed, whereas the other coronins are expressed in a tissue-specific manner: coronins 4 and 5 are expressed in the brain, coronin 6 (cor_{SE}) in epithelial tissues, and coronin 1 in hematopoietic cells (de Hostos, 1999; Parente *et al*., 1999). Although several of the mammalian coronin isoforms are known, for many their physiological roles have not been well defined in macrophages.

Coronins are characterized by the presence of an N-terminal WD repeat domain, separated by a unique region from a coiled coil C-terminal domain (de Hostos, 1999; Gatfield *et al*., 2005). In coronin 1, the N-terminal domain consists of five WD repeats and two additional sequence stretches that are predicted to fold into a seven-bladed β-propeller region (Gatfield *et al*., 2005). WD repeat-containing proteins are involved in a variety of biological processes, ranging from cytoskeletal organization to membrane trafficking to signal transduction (Smith *et al*., 1999), and they may represent a regulatory domain involved in protein–protein interaction, signal transduction, or both.

Mammalian coronin 1, also known as P57 or *T*ryptophan *A*spartate containing *CO*at protein (TACO) is exclusively expressed in leukocytes (Suzuki *et al*., 1995; Ferrari *et al*., 1999). Although in T cells coronin 1 has been suggested to regulate F-actin dynamics, in phagocytic cells, coronin 1 does not affect F-actin–mediated processes (Jayachandran *et al*., 2007). Instead, coronin 1 transiently accumulates at the cytosolic side of nascent phagosomes during phagocytosis (Grogan *et al*., 1997; David *et al*., 1998; Schuller *et al*., 2001; Itoh *et al*., 2002; Foger *et al*., 2006), and it is actively retained during and after internalization of pathogenic mycobacteria, thereby preventing lysosomal delivery (Pieters, 2001; Tailleux *et al*., 2003). In neutrophils, coronin 1 has been suggested to play a role in the control of NADPH oxidase activity by interacting with the soluble component $p40^{phox}$ of the NADPH oxidase (Grogan *et al*., 1997; Allen *et al*., 1999). However, despite many parallels between phagocyte coronin 1 and *Dictyostelium* coronin in localization and dynamics during internalization processes no direct evidence for a role of mammalian coronin 1 in actin-related processes is available.

To analyze a function of coronin 1 in cytoskeletal rearrangement during internalization and locomotion processes, coronin 1-deficient macrophages were generated by RNA interference technology. In mammalian cells short interfer-

This article was published online ahead of print in *MBC in Press* (http://www.molbiolcell.org/cgi/doi/10.1091/mbc.E07–07–0640) on December 27, 2007.

* These authors contributed equally to this work.

Address correspondence to: Jean Pieters (jean.pieters@unibas.ch).

ing RNAs (siRNAs) can be expressed in a stable manner to persistently suppress gene expression (Brummelkamp *et al*., 2002). This allowed the analysis of loss-of-function of coronin 1 in macrophages. As shown in this paper, no defects in actin-mediated processes could be observed in coronin 1 deficient macrophages. However, when macrophages depleted for coronin 1 through RNA interference (RNAi)-mediated gene silencing were infected with pathogenic mycobacteria, the internalized bacilli were rapidly delivered to lysosomes and killed. Together, these data suggest that in J774 macrophages coronin 1 specifically modulates phagosome–lysosome fusion rather than being involved in the regulation of F-actin dynamics.

MATERIALS AND METHODS

DNA Constructs

For siRNA-mediated depletion of coronin 1 in J774 cells, 64-nt oligonucleotides were designed containing a unique 19-nt sequence derived from the target transcript. These were annealed and ligated into the pSUPER vector (OligoEngine) by using BglII/HindIII sites. For selection of J774 clones stably expressing siRNA they were further subcloned together with the H1-RNA promoter as a BamHI/XhoI fragment in the StuI site of the pEGFP-C1 vector (Clontech, Mountain View, CA). The following oligonucleotides have been used for siRNA directed against mouse coronin 1 (siRNAmCORO1nt198-216, target sequence in italics): 5′-GATCCCC*GACTGGACGAGTAGACAAG* TTCAAGA GA*CTTGTCTACTCGTCCAGTC*TTTTTGGAAA-3′ (forward oligonucleotide) and 5′-AGCTTTTCCAAAAA*GACTGGACGAGTAGAC AAG*-TCTCTTGAA*CTT GTCTACTCGTCCAGTC*GGG-3′ (reverse oligonucleotide). As a control, oligonucleotides containing a target sequence from human coronin 1 were designed (siRNAhCORO1nt594-612): 5′-GATCCCC*GCGCGT-GCGCATCAT CGAG*TTCAAGAGA*CTCGATGATGCGCACGCGC*TTTTTGG-AAA-3′ (forward oligonucleotide) and 5′-AGCTTTTCCAAAAA*GCGCGT-GCGCATCATCGAG* TCTCTTGAA*CTCGATGATGCGCACGCGC*GGG-3′ (reverse oligonucleotide). Sequences were verified using the BigDye reagent (PerkinElmer Life and Analytical Science, Boston, MA) on an ABI 310 Sequencer (Applied Biosystems, Foster City, CA) and MacVector software (Accelrys, Munich, Germany).

Antibodies and Immunoblotting

The coding sequence of coronin 1 was fused to the glutathione transferase sequence in the pGEX-4T-1 expression vector, the fusion protein was expressed in *Escherichia coli*, purified, and used for immunization of rabbits to obtain a polyclonal anti-coronin 1 antiserum; anti-peptide antiserum was raised against residues 5-20 of coronin 1 as described in Gatfield *et al*. (2005). Antisera against coronins 2, 3, 6, and 7 were generated using synthetic peptides spanning amino acid residues 428-439 (coronin 2), 419-430 (coronin 3), and 910-922 (coronin 7) as described previously (Ferrari *et al*., 1999). Analysis of protein expression was performed as described previously (Tulp *et al*., 1994; Ferrari *et al*., 1997). The monoclonal anti-tubulin antibody (clone E7) was obtained from the Developmental Studies Hybridoma Bank (University of Iowa, Iowa City, IA). For anti-actin immunoblotting, anti-actin ascites (mouse monoclonal antibody [mAb] clone C4; Chemicon International, Temecula, CA) was used. Detection of coronin 1 and actin was performed using anti-coronin 1 peptide antiserum (1:1000) and anti-actin mAb (1:2000), respectively, followed by goat-anti-rabbit or goat anti-mouse antisera coupled to horseradish peroxidase (Southern Biotechnology Associates, Birmingham, AL) as described previously (Tulp *et al*., 1994). Blots were exposed to x-ray films (Hyperfilm ECL; GE Healthcare, Little Chalfont, Buckinghamshire, United Kingdom) after enhanced chemiluminescence reaction (GE Healthcare).

Mammalian Cell Culture and Transfection

The J774A.1 mouse macrophage-like cell line was grown in DMEM (Invitrogen, Paisley, United Kingdom) and 10% fetal calf serum (Invitrogen). Cells (4×10^6) were transfected by electroporation with 40 μg of circular DNA in a volume of 800 μl in 4-mm cuvettes (570 V, 50 μs; Eppendorf multiporator and buffer system; Eppendorf, Hamburg, Germany). After transfection, stable cell lines expressing siRNA constructs were obtained by selection using 1.2 mg/ml G418 (Invitrogen).

Reverse Transcription-Polymerase Chain Reaction (RT-PCR) of Total Cellular RNA

Total RNA was isolated from 5×10^6 cells of the cell lines J774A.1 and RAW 264.7 by using TRIzol reagent (Invitrogen) in accordance with the manufacturer's protocol. Then, 10 μg of total RNA was subjected to a 30-min treatment at 37°C with DNAse I (Ambion, Austin, TX) to remove contaminating genomic DNA. RNA integrity was then checked using the RNA 6000 Nano Assay kit (Agilent Technologies, Palo Alto, CA). RT reactions were set up according to the manufacturer's protocol with 2 μg of DNAse I-treated total RNA, SuperScript III reverse transcriptase (Invitrogen), and random hexanucleotide primers (Promega, Madison, WI). Polymerase chain reactions using coronin-specific primers and cDNA templates from the RT reactions consisted of 30 cycles of 96°C for 30 s, 56°C for 30 s, and 72°C for 45 s. As a control, PCR reactions were performed concurrently with primers for mouse glyceraldehyde-3-phosphate dehydrogenase (GAPDH). The following primers were used (Okumura *et al*., 1998): coronin-1 forward, 5′-AAACCACTT-GGGACAGTGGCT-3′; coronin-1 reverse, 5′-CATCCGGGCCCAGCGT-CAGCA-3′; coronin-2 forward, 5′-GTGAGCGGTCA GGATGCTAATCCAA-3′; coronin-2 reverse, 5′-TTCTCCCTGCTCCTTGACCAG-3′; coronin-3 forward, 5′-TTTGAGGGGAAGAACGCGGAC-3′; coronin-3 reverse, 5′-AGT-GTCTCCCTCTCTGCCCTC-3′; coronin-4 forward, 5′-CGACTAGGGAT TGTCCTCCA-3′; coronin-4 reverse, 5′-GGTCAGGTGAGGTTTCTCCA-3′; coronin-5 forward, 5′-GATCCCCATCACCAAGAATG-3′; coronin-5 reverse, 5′-GGCTGC CGTCTGTATTGAAG-3′; coronin-6 forward, 5′-GTGCTGGACAT-TGACTGGTG-3′; coronin-6 reverse, 5′-TTGCTTGTGTCCATCTCCTG-3′; coronin-7 forward, 5′-GAGCTGCCAGTGGAGGTACT-3′; and coronin-7 reverse, 5′-GCAACTCATGAC AGCCAGTG-3′. The size of the PCR products is as follows: coronin-1, 430 base pairs; coronin-2, 260 base pairs; coronin-3, 370 base pairs; coronin-4, 297 base pairs; coronin-5, 482 base pairs; coronin-6, 551 base pairs; coronin-7, 600 base pairs; and GAPDH, 450 base pairs.

Immunostaining and Imaging

Cells were grown on 10 well Teflon-coated glass slides (Polysciences, Warrington, PA). After fixation (10 min; 3% paraformaldehyde in phosphate-buffered saline [PBS]; 37°C) and permeabilization in 0.1% saponin/2% bovine serum albumin (BSA) in PBS, cells were incubated for 30 min with primary antibodies (anti-coronin 1 antiserum, 1:4000; anti-tubulin, immunoglobulin G [IgG]1 ascites clone E7, 1:5000). After washing ($3 \times$ 0.1% saponin/2% BSA in PBS), phalloidin-fluorescein isothiocyanate (FITC) (Invitrogen, Carlsbad, CA) and secondary antibodies (goat-anti-mouse Alexa Fluor 633, goat-anti-rabbit Alexa Fluor 568; Invitrogen) were applied for 30 min at 1:200 dilutions. The slides were washed three times with 0.1% saponin/2% BSA in PBS and three times with PBS and mounted using Fluoroguard antifade mounting medium (Bio-Rad, Hercules, CA) and analyzed using an LSM510 Meta confocal laser-scanning microscope (Carl Zeiss, Jena, Germany) and the corresponding software. Video microscopy was performed as described previously (Gatfield *et al*., 2000).

Isolation of Membrane and Cytosol Fractions

To examine subcellular actin distribution biochemically, cells were sedimented at $300 \times g$ for 5 min and resuspended in 10 volumes of homogenization buffer (10 mM triethanolamine, 10 mM acetic acid, 1 mM EDTA, and 0.25 M sucrose, pH 7.4). Homogenization of cells was performed by mechanical disruption using a syringe and 22-gauge needle. The postnuclear supernatant was prepared by centrifugation ($240 \times g$; 15 min; 4°C) and subsequently subjected to ultracentrifugation ($100{,}000 \times g$; 30 min). Membranes (pellet) and cytosol (supernatant) were then analyzed for actin distribution by SDS-polyacrylamide gel electrophoresis (PAGE) and subsequent immunoblotting using anti-actin antibody. Protein equivalents were loaded on SDS-PAGE.

Isolation of a Cytoskeleton-containing Detergent-insoluble Fraction

To isolate a cytoskeleton-containing detergent-insoluble fraction, cells were sedimented at $300 \times g$ for 5 min and resuspended in 10 volumes of ice-cold cytoskeletal isolation buffer (1% Triton X-100 in 80 mM PIPES, pH 6.8, 5 mM EGTA, and 1 mM $MgCl_2$). The samples were then spun in a tabletop centrifuge at $3000 \times g$ for 2 min at 4°C. Pellet and supernatant were analyzed for actin distribution by SDS-PAGE and subsequent immunoblotting using anti-actin antibody. Cell equivalents rather than protein equivalents were loaded on SDS-PAGE.

Analysis of Fluid Phase Uptake and Macropinocytosis by Immunofluorescence

Fluid phase uptake and macropinocytosis were analyzed by seeding macrophages (20,000 cells per well in a 10 well Teflon slide) and allowing these cells to adhere for 4 h in serum-free DMEM at 37°C and 5% CO_2 to induce serum starvation. The cells were then stimulated with 100 nM phorbol 12-myristate 13-acetate (PMA; for fluid phase uptake) or 100 ng/ml epidermal growth factor (Cell Signaling Technology, Danvers, MA; to analyze macropinocytosis) for a period of 20 min at the end of which they were shifted to 4°C and layered with a solution of ice-cold FITC-dextran (140,000 Da; 0.5 mg/ml). The cells were reincubated at 37°C and 5% CO_2 for 20 min to allow uptake of FITC-dextran, shifted to 4°C, fixed with 3% paraformaldehyde, and analyzed using confocal microscopy (LSM510 Meta; Carl Zeiss). The number of FITC-positive vacuoles per cell (n = 20–25) and the percentage of cells having internalized FITC macropinosomes was quantitated (n = 100).

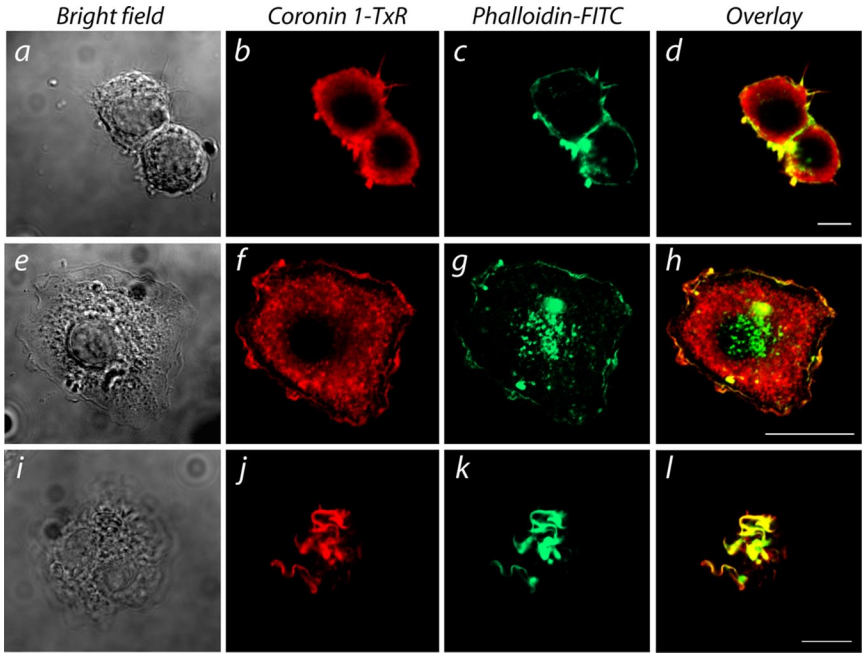

Figure 1. Localization of coronin 1 and F-actin in macrophages. Macrophages (J774) were seeded on coverslips, and they were left untreated (A–D) or activated with 100 nM PMA (E–L). After fixation in 3% paraformaldehyde and permeabilization with 0.1% saponin/2% BSA in PBS, cells were stained with anti-coronin 1 antiserum followed by Texas Red-conjugated secondary antibodies (B, F, and J) or phalloidin-FITC (C, G, and K). Coronin 1 and F-actin colocalized at sites of pseudopod formation (D), at the leading edge (H), and at membrane ruffles (L). Bar, 10 μm.

Analysis of Lamellipodia

Macrophages (20,000 cells in 10% fetal bovine serum [FBS] supplemented DMEM) were seeded per well in a 10-well Teflon slide and allowed to adhere at 37°C and 5% CO_2 for 12 h at the end of which they were stimulated with 10 ng/ml lipopolysaccharide for 1 h, fixed in methanol, and stained for actin by using mouse anti-actin primary antibody and Alexa Fluor 568-tagged anti-mouse secondary. Cells were analyzed using confocal microscopy (LSM510 Meta; Carl Zeiss). The width of the lamellipodia was analyzed using the software provided (n ~ 25).

Quantitative Determination of Phagocytosis by Flow Cytometry

J774 macrophages were grown to 80% confluence in 24-well plates, and then they were shifted to 4°C followed by the addition of yellow-green fluorescent polystyrene beads (FluoSpheres beads, 1 μm in diameter, 1:10,000 dilution of an aqueous 2% suspension; Invitrogen). Next, cells were shifted to 37°C or kept on ice (cold control, to account for particles that are not internalized but merely surface bound) for 30 min, followed by washing in PBS/5% fetal calf serum. Cells were harvested by scraping. Bead uptake was determined by flow cytometry (FACSCalibur; BD Biosciences, San Jose, CA) gating on the live population as assessed by the forward-scatter and side-scatter profiles. Fluorescence-activated cell sorting (FACS) data were analyzed using the FlowJo (Tree Star, Ashland, OR) software package.

Fc Receptor-mediated Phagocytosis of Red Blood Cells (RBCs)

Sheep red blood cells (300 μl of a 10% suspension; Cappel Laboratories/ICN, Durham, NC) were washed twice with PBS, and then they were opsonized by incubation with 1:1000 diluted rabbit-anti-sheep RBC IgG (Cappel Laboratories/ICN) in 1 ml of PBS at room temperature. RBCs were washed three times in PBS and resuspended in DMEM. Opsonized RBCs in ice-cold DMEM were allowed to bind for 15 min to J774 macrophages grown on 10-well Teflon-coated glass slides (Polysciences). We added 800,000 RBCs per 10,000 J774 macrophages.

Unbound RBCs were washed away with ice-cold DMEM. Prewarmed DMEM was added to the slides to initiate phagocytosis of bound RBCs. After 15-min incubation at 37°C and 5% CO_2, slides were exposed to ice-cold distilled water for 15 s to lyse RBCs that were not internalized, washed three times in PBS, and fixed (3% paraformaldehyde in PBS for 10 min at 37°C). To visualize internalized RBCs, slides were stained with rabbit-anti-sheep RBC IgG (diluted 1:2000), phalloidin-FITC, and goat anti-rabbit IgG Alexa Fluor 568 (Invitrogen).

The average number of internalized RBC per J774 macrophage was determined using a fluorescence microscope (LSM510 Meta; Carl Zeiss). Data are means ± SD of three experiments, with 90–130 cells counted in each case.

Complement Receptor-mediated Phagocytosis of RBCs

Three hundred microliters of a 10% suspension of sheep red blood cells (Cappel Laboratories/ICN) were washed twice with PBS and incubated with 1:200 diluted rabbit anti-sheep RBC immunoglobulin M (IgM) (CEDARLANE Laboratories, Burlington, ON, Canada) in 1 ml of PBS at room temperature. RBCs were washed twice in PBS and resuspended in 50 μl of PBS. Fifty microliters of C5-deficient human serum (Sigma Chemie, Deisenhofen, Ger-

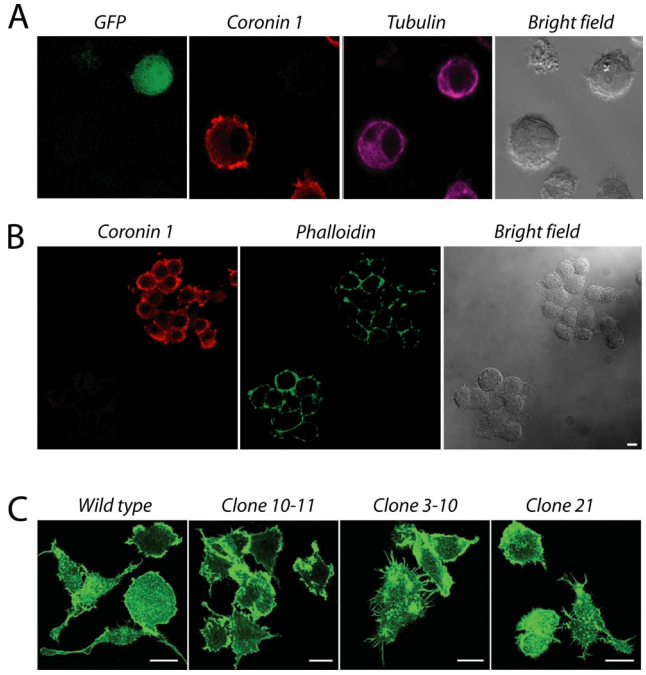

Figure 2. Depletion of coronin 1 by RNA interference. Macrophages (J774) transiently transfected with pEGFP-C1::siRNAmCORO1nt198-216 (A) or pSUPER::siRNAmCORO1nt198-216 (B and C) were seeded on coverslips, fixed, and permeabilized on day 4. Cells were stained for coronin 1 (Texas Red-labeled secondary antibody) and tubulin (Alexa Fluor 633 secondary antibody) (A) or coronin 1 (Texas Red-labeled secondary antibody) and phalloidin-FITC (B). In C, wild-type J774 or the indicated stable clones grown on 10-well Teflon-coated glass slides were activated with 100 nM PMA for 20 min and subsequently stained with phalloidin-FITC to visualize the actin cytoskeleton. Bar, 10 μm.

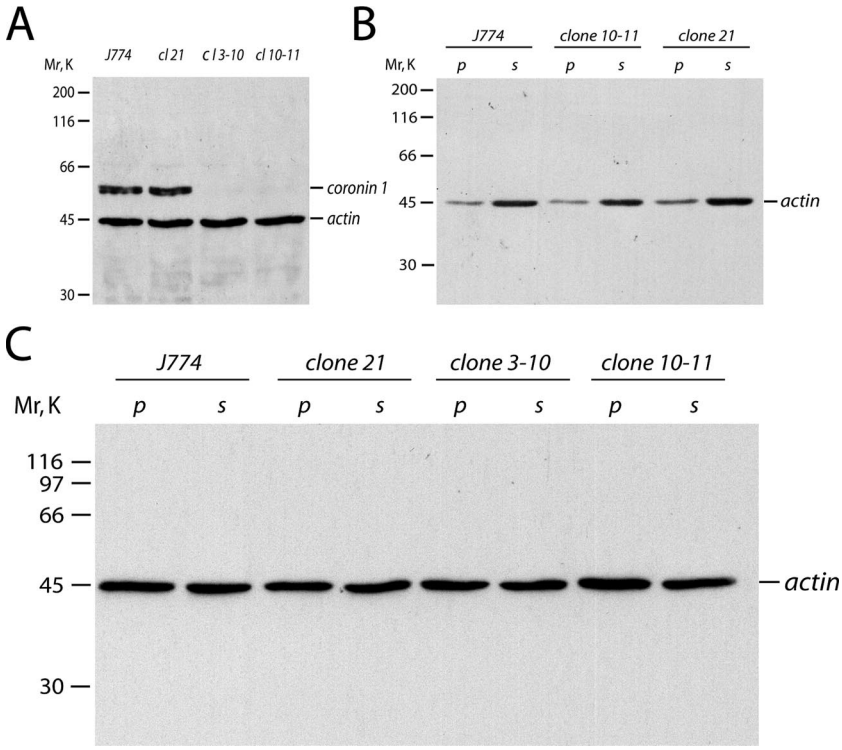

Figure 3. Analysis of J774 cell lines depleted for coronin 1. (A) Equal amounts of wild-type J774 macrophages or the indicated stably transfected cells were lysed in Laemmli sample buffer, and coronin 1 expression was analyzed by immunoblotting after SDS-PAGE by using anti-coronin 1 and anti-actin antibodies. Clones 3–10 and 10–11 express pEGFP-C1::siRNAm CORO1nt198-216; clone 21 expresses the control construct pEGFP-C1::siRNAhCORO1nt 594-612. (B) Wild-type J774 macrophages or the indicated stable clones were homogenized, and the postnuclear supernatant was subjected to ultracentrifugation (100,000 × *g* for 30 min). Actin distribution between membranes (pellet, p) and cytosol (supernatant, s) was analyzed by SDS-PAGE and subsequent immunoblotting by using anti-actin antibody. Protein equivalents were loaded on SDS-PAGE. (C) Analysis of actin distribution between a Triton X-100–insoluble fraction (p) and cytosol (s) by immunoblotting as described in *Materials and Methods*.

many) were added, and the RBC suspension was incubated for 20 min at 37°C. RBCs were washed again three times in PBS, and then they were resuspended in DMEM. J774 macrophages grown on 10-well Teflon-coated glass slides (Polysciences) were serum starved for 2 h in DMEM at 37°C and 5% CO_2, and they were activated with 100 nM PMA in DMEM for 20 min. Subsequently, 800,000 RBCs were added per 10,000 J774 macrophages, and phagocytosis was allowed to occur for 1 h at 37°C and 5% CO_2. Slides were exposed to ice-cold distilled water for 15 s to lyse RBCs that were not internalized, they were washed three times in PBS, and then they were fixed (3% paraformaldehyde in PBS for 10 min at 37°C). To visualize internalized RBCs, slides were stained as described above.

The average number of internalized RBC per J774 macrophage was determined using a fluorescence microscope (LSM510 Meta; Carl Zeiss). Data are means ± SD of three experiments, with 30–50 cells counted in each case.

Determination of Superoxide Production

J774 macrophages (1×10^6) resuspended in 1 ml of 10% DMEM were either treated with DMSO or 100 nM PMA for 30 min at the end of which they were treated with reactive oxygen species indicator 2,7-dichlorodihydrofluorescein diacetate (Invitrogen) at 1.5 μM concentration for 15 min. The cells were washed twice in 10 ml of PBS containing 2% FBS and resuspended in 1 ml of the same and analyzed using FACSCaliber (BD Biosciences) with excitation at 488 nm and emission measured at FL-1.

Cell Migration Assay

Macrophages were harvested, washed twice with DMEM/10 mM HEPES, pH 7.3, and seeded at a density of 4×10^5 cells/well into the upper part of the Transwell chamber (8-μm pore size, 6.5 mm in diameter; Corning Life Sciences, Acton, MA) containing 0.6 ml of DMEM/10 mM HEPES, pH 7.3, with or without chemoattractant (either 200 ng/ml macrophage chemoattractant protein 1 or 10% zymosan-activated human serum) in the lower well. As a control, the cells were treated with 4 μM latrunculin B. After 4 h of incubation at 37°C, the Transwell filters were fixed in 3% paraformaldehyde and wiped on the top with a cotton swab to remove nonmigrated cells. Filter membranes were stained with propidium iodide solution (2 μg/ml PBS), excised, and mounted onto glass slides using Fluoroguard antifade mounting medium (Bio-Rad). Migrated cells were counted in five to eight optical fields per filter by using a confocal microscope (LSM510 Meta; Carl Zeiss) at 63× magnification.

Mycobacterial Survival

Mycobacterial survival was essentially performed as described previously (Walburger *et al*., 2004). In brief, 5×10^4 J774 cells in 200 μl of DMEM supplemented with 10% FBS was seeded per well in a 96-well plate (Corning Life Sciences), and they were allowed to adhere for 2 h at 37°C and 5% CO_2. Then, 100 μl of *Mycobacterium bovis* bacillus Calmette-Guérin (BCG) washed three times in fresh DMEM resuspended to a final OD of 0.02 was replaced gently over the adhered cells, and it was allowed to infect the macrophages for 1 h at 37°C and 5% CO_2. Free bacteria were removed by three washes and treatment with 200 μg/ml amikacin for 1 h. To initiate the chase, 200 μl of fresh medium was added per well and chased for the times indicated. At the end of chase, the medium was removed, and the macrophages were lysed by addition of 100 μl of incorporation media (7H9 medium with 10% DS supplement, 0.15% saponin, and 10 μCi/ml tritiated uracil) to release the intracellular mycobacteria, and then the macrophages were further incubated for 24 h at 37°C and 5% CO_2. Mycobacteria were lysed by addition of 20 μl of 1 N NaOH and incubation at 50°C for 30 min. Proteins from the lysate were precipitated with 80 μl of 50% trichloroacetic acid, and the supernatant was harvested using a FilterMate harvester (PerkinElmer Life and Analytical Sciences) with Unifilter-96, GF/C filter. The incorporated counts were measured using a TopCount microplate scintillation counter (PerkinElmer Life and Analytical Sciences) according to the manufacturer's protocol.

RESULTS

Coronin 1 Localization in Resting and Activated J774 Macrophages

In *Dictyostelium*, coronin colocalizes with actin at crown-shaped structures at the leading edge of the cell, and in phagocytic cups and macropinosomes (de Hostos *et al*., 1991; Maniak *et al*., 1995). To analyze the localization of coronin 1 in J774 macrophages, cells were analyzed by immunofluorescence microscopy. Coronin 1 strongly colocalized with F-actin in pseudopods of resting J774 macrophages (Figure 1D), lamellipodia/leading edges (Figure 1H), and membrane ruffles (Figure 1L) that extend from the upper part of PMA-activated cells. Thus, coronin 1 is enriched in structures where the F-actin cytoskeleton is being remodeled similarly to the localization of coronin in *Dictyostelium*.

Establishing RNA Interference Technology in J774 Macrophages

To address a function for coronin 1 in actin-related processes in J774 macrophages, coronin 1 expression was ablated using

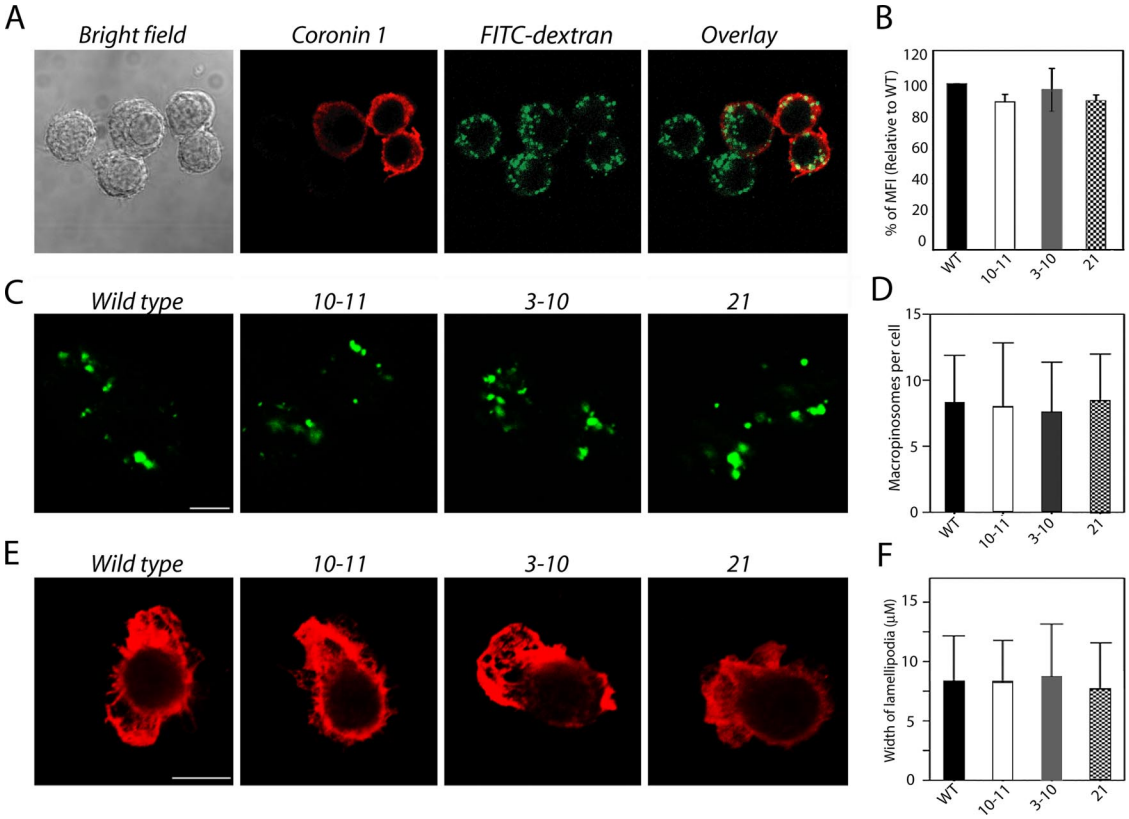

Figure 4. Fluid phase uptake, macropinocytosis and lamellipodia formation in coronin 1-depleted macrophages. (A) Immunofluorescence analysis of transiently siRNA-transfected J774 cells (day 4) incubated with the fluid phase marker FITC-dextran (2 mg/ml; 70,000 Da) for 20 min. Cells were stained with anti-coronin 1 antibody (Texas Red-labeled secondary antibody). (B) Flow cytometric analysis of bead uptake by stable siRNA-expressing J774 cells. Wild-type (WT), coronin 1-depleted (clones 3–10 and 10–11), or control J774 clones (clone 21) were incubated for 30 min with yellow-green fluorescent polystyrene beads as described in *Materials and Methods*. Bead uptake was quantified by determining the mean fluorescent intensity (MFI) of the living population (n = 10,000). MFI of the cold controls is subtracted from the MFI of the 37°C samples, and MFI for J774 WT cells is set to 100%. MFI for the indicated clones is expressed in percentage relative to WT. Data are means ± SD from three independent experiments. (C) Macropinosome formation in stably transfected J774 clones incubated with the fluid phase marker FITC-dextran (0.5 mg/ml; 140,000 Da) for 20 min in the presence of epidermal growth factor. (D) Quantitation of the number of macropinosomes per cell as analyzed by confocal microscopy upon stimulation with EGF (n = 25 ± SD). (E) Analysis and (F) quantitation of the lamellipodia width in various J774 clones (n = 25 +/− SD).

RNA interference technology. Analysis of the stability of coronin 1 mRNA translation products by pulse labeling of J774 cells revealed that coronin 1 is stable over several days (data not shown). To analyze down-regulation of coronin 1, cells were transfected with the siRNA constructs expressing the murine coronin 1-specific sequences together with the enhanced green fluorescent protein (pEGFP-C1::siRNAmCORO1nt198-216; see *Materials and Methods*), and they were analyzed after 4 d for the presence of coronin 1. As shown in Figure 2A, complete down-regulation of coronin 1 translation was achieved at the single cell level (in ~5% of total cells). In J774 cells that had been transfected with siRNA constructs specific for human coronin 1 (pEGFP-C1::siRNAhCORO1nt594-612), no coronin 1-depleted cells were observed (data not shown). Down-regulation of coronin 1 affected neither the overall cellular morphology nor the tubulin cytoskeleton (Figure 2A). To analyze whether depletion of coronin 1 affects cytoskeletal structures such as the cortical actin cytoskeleton at the single cell level, J774 macrophages transiently transfected with pSUPER::siRNAmCORO1nt198-216 were fixed, permeabilized, and stained for F-actin. Neither the overall morphology of the cells, nor the F-actin cortical structures showed an

Table 1. EGF induced macropinosomes in J774 cells

J774	% of cells positive for macropinosomes
WT	65.4
10–11	69.7
3–10	67.8
21	65

Table 2. Migration speed of J774 WT and siRNA clones

J774	Migration speed (μm/30 min) ± SEM
WT	14.304 ± 3.058
10–11	12.95 ± 1.033
3–10	13.236 ± 1.887
21	13.804 ± 1.283

n = 8–12 cells/cell type.

altered morphology upon coronin 1 depletion (Figure 2B). Additionally, J774 macrophages that were depleted for coronin 1 (stable clones 3–10 and 10–11; see below) were equally capable to spread on glass slides and form pseudopods compared with nondepleted cells (Figure 2C). Together, these data indicate that coronin 1 is not required for cortical F-actin colocalization or pseudopod formation upon cell spreading of J774 macrophages.

Generation of Stable Coronin 1-deficient Macrophage Cell Lines

To establish cell lines that are permanently depleted for coronin 1, J774 macrophages were transfected with expression vectors expressing the enhanced green fluorescent protein (EGFP) and the murine or human siRNA sequences (see *Materials and Methods*). Two coronin 1 negative clones were selected (clones 3–10 and 10–11; pEGFP-C1::siRNAmCORO1nt198-216) and a control clone (clone 21; pEGFP-C1::siRNAhCORO1nt594-612). To analyze the degree of down-regulation, equal cell numbers were lysed in Laemmli sample buffer, and the coronin 1 levels were analyzed by immunoblotting. Although clone 21 expressed coronin 1 levels similar to wild-type J774 cells, in clone 3–10 and 10–11, no coronin 1 could be detected (Figure 3A). As a control, the levels of actin were analyzed, which were identical for coronin 1-depleted and control cells, indicating that depletion of coronin 1 does not have an effect on the total levels of actin.

To analyze the association of actin with membranes in coronin 1-deficient J774 macrophages, cells were homogenized, and the postnuclear supernatant was separated by sedimentation into a membrane and a cytosolic fraction. SDS-PAGE followed by immunoblotting using anti-actin antibody showed identical patterns of distribution for coronin 1-negative (clones 3–10 and 10–11) and coronin 1-positive (clones 21 and J774) cell lines (Figure 3B), demonstrating that the absence of coronin 1 does not affect steady state actin association with the membrane. To further investigate potential changes in the actin polymerization state due to coronin 1 depletion, the cytoskeleton was isolated by cell lysis in 1% Triton X-100 and low-speed centrifugation (3000 $\times$ *g* for 2 min). Pellet and supernatant were analyzed by immunoblotting by using anti-actin antibody. Actin was found to be equally distributed between the insoluble and the soluble fraction for coronin 1-negative (clones 3–10 and 10–11) and coronin 1-positive (clone 21 and J774) cell lines (Figure 3C).

Fluid Phase Uptake, Macropinocytosis, and Lamellipodia Formation in the Absence of Coronin 1

Fluid phase uptake including macropinocytosis ensures the internalization of nonparticulate material in an actin-dependent process (Maniak *et al*., 1995; Steinman and Swanson, 1995; Araki *et al*., 1996; Amyere *et al*., 2000; Johannes and Lamaze, 2002). To analyze a role for coronin 1 in fluid phase uptake and macropinocytosis, coronin 1-depleted or control J774 macrophages that were transiently transfected with pSUPER::siRNAmCORO1nt198-216 and pSUPER::siRNAhCORO1nt594-612, respectively, were in-

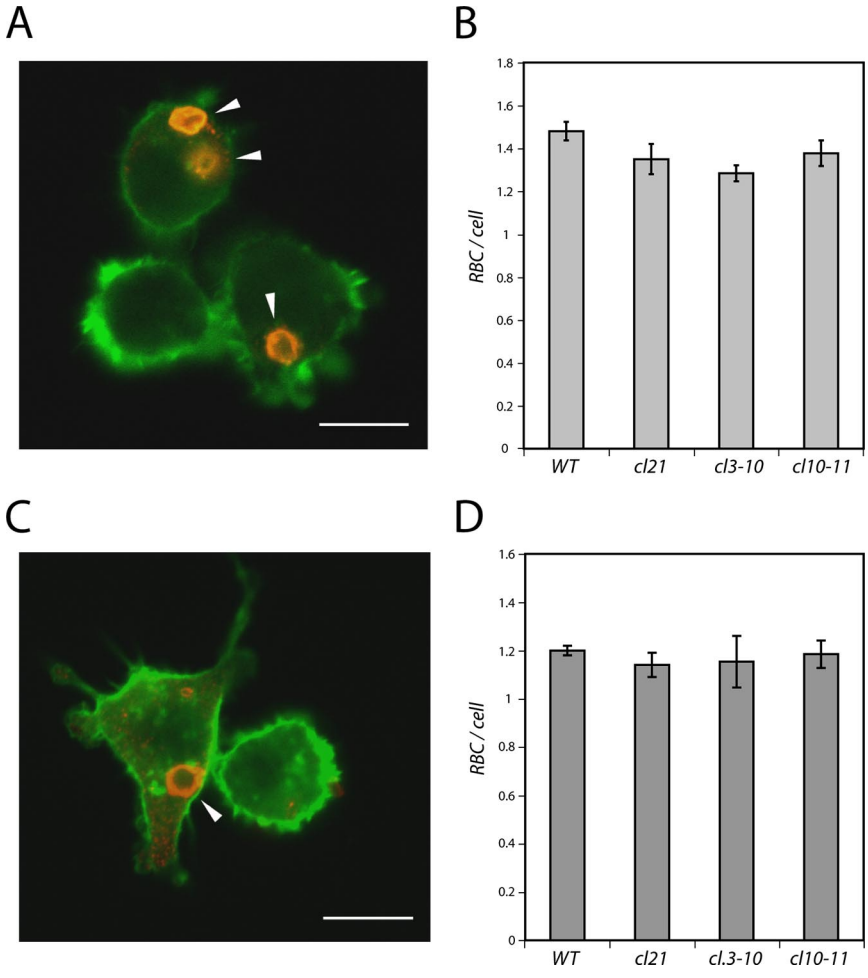

Figure 5. Phagocytosis of RBCs. Sheep RBCs were either IgG opsonized (A and B) or complement treated (C and D), and they were allowed to be phagocytosed by J774 macrophages as described in *Materials and Methods*. RBCs were stained with rabbit-anti-sheep RBC IgG and goat-anti-rabbit IgG Alexa Flour 568. The actin cytoskeleton was visualized using phalloidin-FITC. (A) Representative image of IgG-opsonized RBCs internalized by J774 WT macrophages. RBCs are in red, and phalloidin-stained J774 cells are in green. (B) Results from determining the average number of internalized, IgG-opsonized RBCs per macrophage. Ninety to 130 cells were counted, and data are means ± SD from three independent experiments. (C) Representative image of complement-treated RBCs internalized by J774 WT macrophages. RBCs are in red, and phalloidin-stained J774 cells are in green. (D) Quantitation of the average number of internalized, complement-treated RBCs per macrophage. Thirty to 50 cells were counted, and data are means ± SD from three independent experiments. Bar, 10 μm. Arrowhead, internalized RBCs.

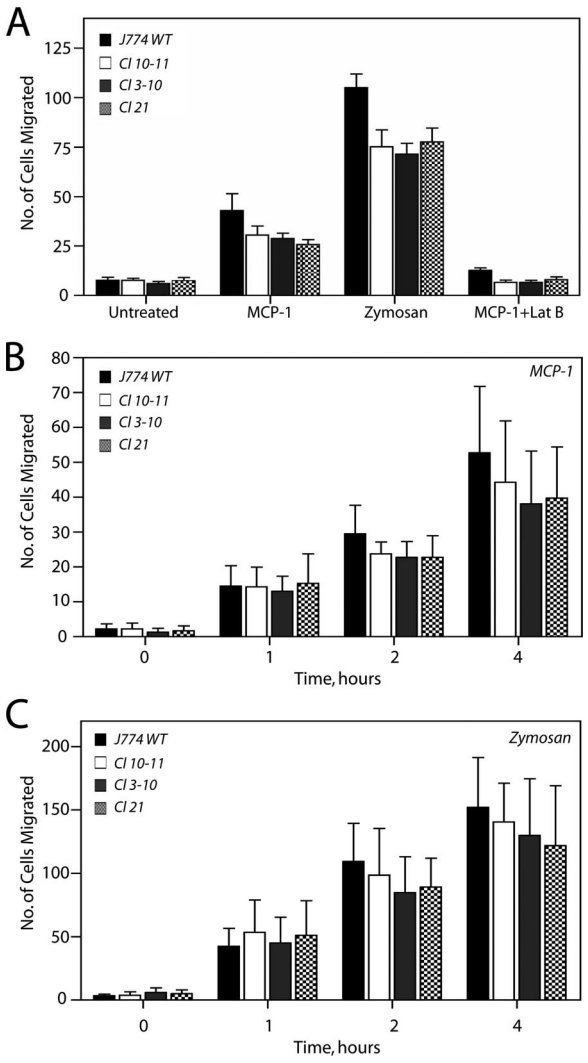

Figure 6. Chemotaxis in coronin 1-depleted macrophages. Coronin 1-depleted or control J774 clones were placed in the upper well of a Transwell assay plate (8-μm pore size, 6.5 mm in diameter), and they were subjected to a gradient of 10% zymosan-activated human serum or 200 ng/ml MCP-1 in culture media placed in the lower well for 4 h (A) or for 0, 1, 2, and 4 h (B and C). In A, the control conditions contained medium only (untreated) in the lower well or cells treated with 4 μM latrunculin B (Lat B). Cells that had traversed the filter were stained with propidium iodide and quantitated microscopically. Experiments were done in duplicate, and three to five fields were analyzed per filter.

cubated with the fluid phase marker FITC-dextran for 20 min after activation with PMA, and the number of FITC-dextran–positive vesicles per cell and the percentage of cells with macropinosomes were analyzed. As seen in Figure 4A, no differences were observed in fluid phase uptake between coronin 1-negative and -positive cells. To analyze macropinocytosis in the presence and absence of coronin 1, coronin 1-expressing or -depleted cells were stimulated with the epidermal growth factor (EGF) before incubation with FITC dextran. As shown in Figure 4, C and D, and Table 1, no qualitative and quantitative differences were observed in the appearance and number of macropinosomes in either coronin 1-expressing and coronin 1-depleted macrophages.

The formation of cellular protrusions such as lamellipodia is spatially controlled by actin polymerization (Pantaloni *et al*., 2001). To determine whether coronin 1 plays a role in the formation of lamellipodia, coronin 1-expressing and coronin 1-depleted cells were allowed to spread on glass slides, and the dimensions of the lamellipodia formed were quantitated after staining with anti-actin antibodies. No differences in the appearance of lamellipodia were observed between coronin 1-positive and -negative macrophages (Figure 4, E and F; see also Supplemental Movies 1–4), suggesting that coronin 1 is dispensable for this actin-based process.

To analyze the kinetics of motility in the presence and absence of coronin 1, migration speed was quantitated from the accompanying video sequences (Supplemental Movies 1–4). As shown in Table 2, no differences were apparent between the different cell lines.

Phagocytosis in the Presence and Absence of Coronin 1

To analyze the contribution of coronin 1 to phagocytosis, macrophage cell lines stably depleted for coronin 1 were incubated with nonopsonized fluorescent polystyrene beads for 30 min, and the degree of phagocytosis was determined using FACS analysis (Figure 4B). Whereas nontransfected J774 cells had a slightly higher capacity to phagocytose, the coronin 1-depleted clones 3–10 and 10–11 showed a similar capacity for phagocytosis compared with the J774 cell line stably expressing siRNA for human coronin 1 (clone 21). In addition, the kinetics of phagocytosis of polystyrene beads was assessed by time-lapse imaging (Supplemental Videos 5–8). No differences were apparent between coronin 1-expressing and -depleted macrophages. Together, these data demonstrate that coronin 1 is not involved in phagocytosis of nonopsonized polystyrene beads.

The initial event in the phagocytosis of particles is recognition of the particle by specific receptors on the plasma membrane of the phagocytes (Aderem and Underhill, 1999). To analyze a possible role for coronin 1 in receptor-mediated phagocytosis, J774 wild-type and coronin 1-depleted cells (clones 3–10 and 10–11) were incubated with sheep RBCs. Subsequently, the average number of internalized RBCs per cell was determined by immunofluorescence microscopy. Although IgG-opsonized RBCs served as cargo for Fc receptor-mediated phagocytosis, treatment of RBCs with rabbit anti-sheep RBC IgM and C5-deficient human serum allowed us to study complement receptor (CR)-mediated uptake. Neither Fc receptor (Figure 5B) nor CR-mediated uptake (Figure 5D) was found to be affected by RNAi-mediated depletion of coronin 1. Therefore, we conclude that coronin 1 is not required for receptor-mediated uptake of sheep RBCs.

Macrophage Cell Locomotion and Chemotaxis in the Absence of Coronin 1

Coronin is critically involved in chemotaxis in *Dictyostelium* (de Hostos *et al*., 1993). To analyze a role for coronin 1 in chemotaxis in J774 macrophages, coronin 1-deficient J774 macrophages were placed in the upper reservoir of a Transwell chamber, and they were subjected to a chemotactic gradient from the lower chamber containing either 10% zymosan-activated human serum or 200 ng/ml monocyte chemoattractant protein-1 (MCP-1) in cell culture medium. Alternatively, the lower chamber contained medium alone (no gradient) or cells treated with actin-depolymerizing agent latrunculin B serving as internal controls. Chemotaxis was assessed by analyzing the number of cells that had traversed the filter by staining with propidium solution either after 4 h (Figure 6A) or by analysis after 1, 2, and 4 h

Table 3. NADPH oxidase activity in coronin 1-depleted macrophages

	Mean fluorescence value	
J774	Basal	PMA (200 nM)
WT	274	1894
10–11	264	1640
3–10	255	1778
21	316	1715

(Figure 6, B and C). As shown in Figure 6, A–C, although the siRNA expression slightly reduced the chemotactic activity of macrophages independently of coronin 1, coronin 1-depleted and the control siRNA macrophages (clone 21) displayed similar chemotactic activity, suggesting that coronin 1-deficient J774 macrophages were not adversely affected in cell locomotion as induced by chemotactic stimuli.

NADPH Oxidase Activity in the Absence of Coronin 1 in J774 Macrophages

Coronin 1 has been suggested to function as an inhibitor of the superoxide-generating NADPH oxidase by sequestration of the soluble enzyme subunit $p40^{phox}$ (Grogan *et al.*, 1997). To analyze the capacity of coronin 1 to regulate NADPH oxidase activity, coronin 1-deficient and control macrophage cell lines were assayed for constitutive and stimulated superoxide production by incubation with the chromogenic substrate 2,7-dichlorodihydrofluorescein diacetate in the presence or absence of PMA. Superoxide production in resting and PMA-stimulated cells was not influenced by the presence or absence of coronin 1, excluding a role for coronin 1 in the regulation of NADPH oxidase activity (Table 3).

Mycobacterial Trafficking and Survival in Coronin 1-negative J774 Macrophages

Although coronin 1 was dispensable for the above-mentioned F-actin–dependent processes in J774 cells, upon mycobacterial uptake coronin 1 is retained around phagosomes, thereby blocking phagosome lysosome fusion (Ferrari *et al.*, 1999). To analyze whether mycobacterial trafficking is affected in J774 cells lacking coronin 1 expression, cells were infected with *M. bovis* BCG for 1 h, followed by a 3-h chase. As shown in Figure 7, A and B, although in J774 cells expressing the control siRNA construct the mycobacteria remained outside lysosomes, in coronin 1-negative macrophages mycobacteria were largely transported to lysosomes, to a similar degree as *M. bovis* BCGΔ*pkng*, a mycobacterial mutant that lacks the capacity to withstand lysosomal delivery (Walburger *et al.*, 2004; Nguyen *et al.*, 2005; Scherr *et al.*, 2007). As expected, on the basis ofthe intracellular localization of mycobacteria in the coronin 1-negative cell lines, the proliferation of mycobacteria was severely affected. Whereas

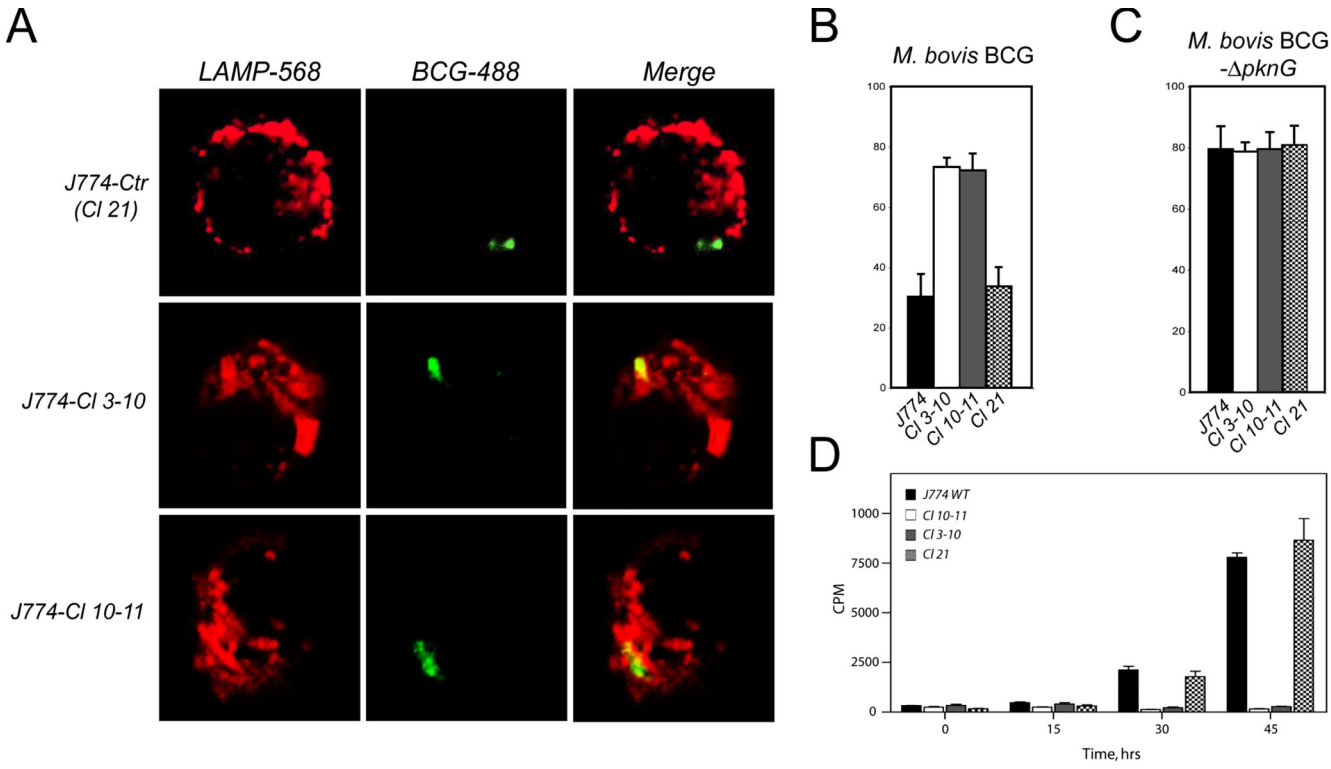

Figure 7. Trafficking and survival in wild-type and coronin 1-depleted macrophages. (A) Macrophages were infected with *M. bovis* BCG, chased for 3 h, and then fixed with methanol and stained for lysosome-associated membrane protein (LAMP)1 (568) or mycobacteria (488). Cells were analyzed by confocal microscopy. (B and C) Quantitation of the lysosomal delivery of wild-type or PknG-deficient *M. bovis* BCG in the different macrophage clones indicated as determined by confocal microscopy (n ~ 150). The error bars represent the SD values from three independent experiments. (D) Survival of mycobacteria in the macrophage clones indicated as determined by incorporation of tritiated uracil. The error bars represent SD values from triplicate values, and the data shown are representative of at least three independent experiments.

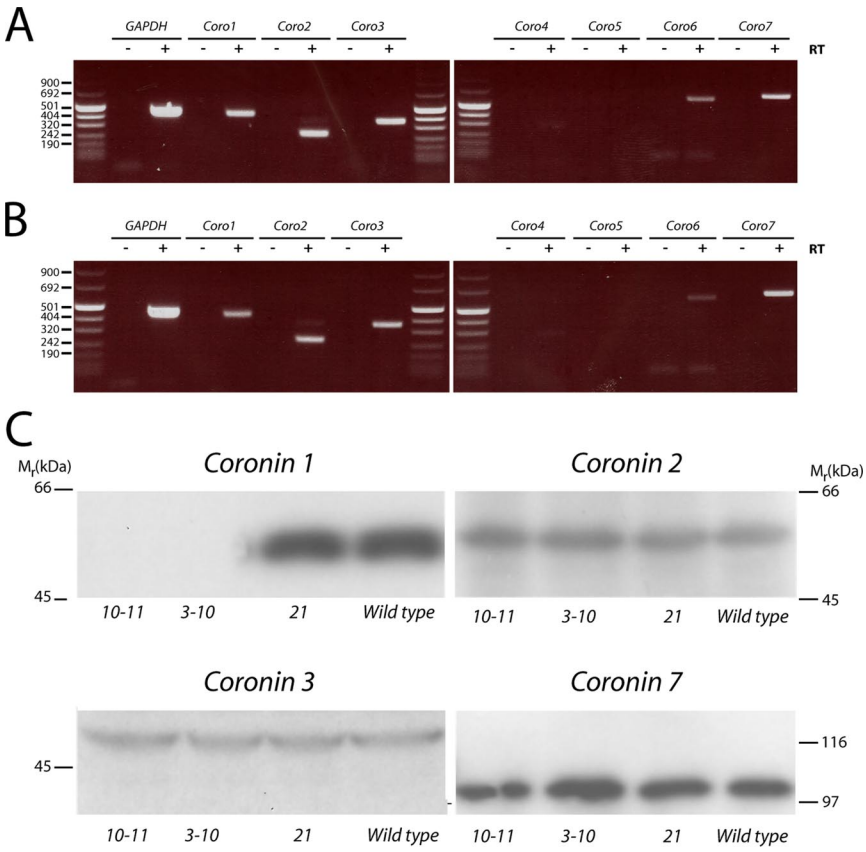

Figure 8. Expression of coronin 1-7 in cell lines as determined by RT-PCR. Total RNA was extracted from J774 and RAW264.7 macrophages, reversely transcribed, and analyzed for the presence of coronin 1-7 transcripts by PCR. Expression of coronin 1-7 in J774 (A) and RAW264.7 (B) cells. RT, reverse transcriptase. For immunoblotting, equal cell numbers were loaded per well from the cell lines indicated in C after denaturation in Laemmli sample buffer. Blots were probed for the coronin isoforms indicated using anti-tubulin antibodies as a control.

in control J774 cells, mycobacteria readily survived and proliferated, in the absence of coronin 1 expression mycobacteria failed to proliferate, similar to mycobacteria lacking the essential intracellular survival factor PknG (Figure 7D). Together, these data indicate that coronin 1 specifically modulates the intracellular transport of pathogenic mycobacteria.

Analysis of the Expression of Coronin Family Members

The lack of any obvious phenotype of coronin 1-negative J774 macrophages could be explained by the expression of several coronin homologues within J774 macrophages. Therefore, the expression of the seven coronin homologues that have been so far described to be present in mammalian cells (Rybakin and Clemen, 2005) was assessed by RT-PCR. As shown in Figure 8, coronins 1, 2, 3, 6, and 7 were found to be expressed in the macrophage cell lines J774 and RAW264.7, whereas coronins 4 and 5 were not expressed in these cell types. Consistent with these results, no coronin 4 or 5 was detected by immunoblotting by using the lysates of coronin 1-expressing or -depleted cells. In addition, we were unable to detect a specific signal using antisera raised against coronin 6 (data not shown). However, as shown in Figure 8C, the amounts of coronins 2, 3, and 7 were unaltered upon coronin 1 depletion, suggestion that coronin 1 depletion did not result in the modulation of the expression of these other coronin isoforms.

DISCUSSION

The WD repeat-containing family of mammalian coronins has been implicated in various actin-related processes, on the basis of the homology with *Dictyostelium* coronin and the capacity of in *E. coli*-expressed coronins to interact with actin in vitro. To analyze a role for coronin 1, also known as P57 or TACO in actin-related processes in macrophages, we have generated cell lines depleted for coronin 1 by RNA interference. Coronin 1-depleted cells displayed a normal morphology, and they were indistinguishable from wild-type cells with respect to the actin and tubulin cytoskeletal structures, lamellipodia formation, spreading, migration, phagocytosis, and macropinocytosis. Furthermore, chemotaxis and the activity of the NADPH oxidase was normal. However, when macrophages depleted for coronin 1 by RNAi interference were infected with pathogenic mycobacteria, all bacilli were transferred to lysosomes and killed, in contrast to the phagosomal residence and survival of mycobacteria phagocytosed by control macrophages. We conclude that in macrophage cell lines coronin 1 is fully dispensable for F-actin based processes but specifically mediates the intracellular survival of mycobacteria by blocking phagosome–lysosome fusion.

The data presented here are in sharp contrast to recent work claiming a role for coronin 1 in phagocytosis on the basis of TAT-mediated transduction of the coronin 1 WD domain (Yan *et al*., 2005). However, in our hands, expression of exclusively the coronin 1 WD domain, either alone or as a fusion protein, resulted in aggregation of the resulting product due to misfolding in the absence of the C-terminal region (Gatfield *et al*., 2005; data not shown). Therefore, the observed reduction by Yan *et al*. (2005) might result from expressing or transducing misfolded proteins inside J774 macrophages, which may compromise cellular functions such as spreading, membrane ruffling, and phagocytosis.

Notably, the results presented here, as far as we know, provide the first description of macrophage cell lines derived using RNAi technology in which a complete gene knockdown has been achieved. In addition, the phenotype of the RNAi-mediated coronin 1-depleted macrophage cell lines are fully consistent with the phenotype of macrophages derived from coronin 1-deficient mice (Jayachandran *et al*., 2007), excluding any artifacts introduced into the experimental system either through RNAi-mediated down-regulation or gene-targeting technology.

In J774 macrophages, several other coronins are expressed, such as the ubiquitously expressed coronin 2 and 3 molecules; therefore, the function of coronin 1 for the above-mentioned actin-mediated activities might be redundant with these other coronin family members. Interestingly, the yeast *Saccharomyces cerevisiae* expresses only a single coronin gene (*crn1*), and deletion of the coronin gene does not have an obvious phenotype (Heil-Chapdelaine *et al*., 1998; Goode *et al*., 1999). The yeast coronin protein interacts with the actin-related protein 2/3 (Arp2/3) complex; therefore, it may be involved in the temporal and spatial organization of actin filamentous networks (Humphries *et al*., 2002). Whether coronin molecules in leukocytes regulate actin filamentous network under specific physiological conditions remains to be established.

What may be the role of coronin 1 in macrophages? One possibility is that coronin 1 functions in the temporal and spatial regulation of the actin cytoskeleton, as was suggested from analysis of T cells from coronin 1-deficient mice (Foger *et al*., 2006). Given the lack of any phenotype with respect to the actin-related processes investigated in this study, the involvement of coronin 1 may be restricted to specific conditions (Gatfield and Pieters, 2000). Such conditions may include the internalization and intracellular processing of certain pathogens or the internalization of leukocyte specific cell surface receptors (Nal *et al*., 2004). For example, when pathogenic microbes such as *Mycobacterium* spp. and *Helicobacter pylori* enter macrophages, they recruit and retain coronin 1 around the nascent phagosome, thereby preventing fusion of phagosomes with lysosomes (Ferrari *et al*., 1999; Zheng and Jones, 2003). Given a possible role of actin in regulating membrane transport processes (Guerin and de Chastellier, 2000; Vieira *et al*., 2002), coronin 1 actively recruited by these pathogens may be involved in the modulation of the actin cytoskeleton thereby influencing intracellular trafficking and survival.

In conclusion, the data presented here show that coronin 1 depletion in J774 macrophages does not influence actin-dependent processes unlike coronin from *Dictyostelium*, such as phagocytosis, cell motility, or regulation of NADPH oxidase activity. Instead, coronin 1 was specifically required to allow mycobacteria to escape lysosomal delivery and to survive intracellularly. However, the results presented here do not provide a clue as to the normal role for coronin 1 in the absence of a mycobacterial infection. Coronin 1 may be involved in as yet unknown leukocyte-specific processes, and the availability of coronin 1-negative cell lines described in this study may be instrumental in addressing a function for coronin 1 in these important leukocytes.

ACKNOWLEDGMENTS

We thank Anna Melone for the generation and analysis of macrophages expressing coronin 1-fluorescent protein fusions. This work was supported by grants from the Swiss National Science Foundation, the World Health Organization, and the Swiss Life Jubilaeumsstiftung (to J.P.).

REFERENCES

Aderem, A., and Underhill, D. M. (1999). Mechanisms of phagocytosis in macrophages. Annu. Rev. Immunol. *17*, 593–623.

Allen, L. A., DeLeo, F. R., Gallois, A., Toyoshima, S., Suzuki, K., and Nauseef, W. M. (1999). Transient association of the nicotinamide adenine dinucleotide phosphate oxidase subunits p47phox and p67phox with phagosomes in neutrophils from patients with X-linked chronic granulomatous disease. Blood *93*, 3521–3530.

Amyere, M., Payrastre, B., Krause, U., Van Der Smissen, P., Veithen, A., and Courtoy, P. J. (2000). Constitutive macropinocytosis in oncogene-transformed fibroblasts depends on sequential permanent activation of phosphoinositide 3-kinase and phospholipase C. Mol. Biol. Cell *11*, 3453–3467.

Araki, N., Johnson, M. T., and Swanson, J. A. (1996). A role for phosphoinositide 3-kinase in the completion of macropinocytosis and phagocytosis by macrophages. J. Cell Biol. *135*, 1249–1260.

Brummelkamp, T. R., Bernards, R., and Agami, R. (2002). A system for stable expression of short interfering RNAs in mammalian cells. Science *296*, 550–553.

David, V., Gouin, E., Troys, M. V., Grogan, A., Segal, A. W., Ampe, C., and Cossart, P. (1998). Identification of cofilin, coronin, Rac and capZ in actin tails using a *Listeria* affinity approach. J. Cell Sci. *111*, 2877–2884.

de Hostos, E. L. (1999). The coronin family of actin-associated proteins. Trends Cell Biol. *9*, 345–350.

de Hostos, E. L., Bradtke, B., Lottspeich, F., Guggenheim, R., and Gerisch, G. (1991). Coronin, an actin binding protein of *Dictyostelium discoideum* localized to cell surface projections, has sequence similarities to G protein beta subunits. EMBO J. *10*, 4097–4104.

de Hostos, E. L., Rehfuess, C., Bradtke, B., Waddell, D. R., Albrecht, R., Murphy, J., and Gerisch, G. (1993). *Dictyostelium* mutants lacking the cytoskeletal protein coronin are defective in cytokinesis and cell motility. J. Cell Biol. *120*, 163–173.

Ferrari, G., Knight, A. M., Watts, C., and Pieters, J. (1997). Distinct intracellular compartments involved in invariant chain degradation and antigenic peptide loading of major histocompatibility complex (MHC) class II molecules. J. Cell Biol. *139*, 1433–1446.

Ferrari, G., Langen, H., Naito, M., and Pieters, J. (1999). A coat protein on phagosomes involved in the intracellular survival of mycobacteria. Cell *97*, 435–447.

Foger, N., Rangell, L., Danilenko, D. M., and Chan, A. C. (2006). Requirement for coronin 1 in T lymphocyte trafficking and cellular homeostasis. Science *313*, 839–842.

Gatfield, J., Albrecht, I., Zanolari, B., Steinmetz, M. O., and Pieters, J. (2005). Association of the leukocyte plasma membrane with the actin cytoskeleton through coiled coil-mediated trimeric coronin 1 molecules. Mol. Biol. Cell *16*, 2786–2798.

Gatfield, J., and Pieters, J. (2000). Essential role for cholesterol in entry of mycobacteria into macrophages. Science *288*, 1647–1650.

Gerisch, G., Albrecht, R., De Hostos, E., Wallraff, E., Heizer, C., Kreitmeier, M., and Muller Taubenberger, A. (1993). Actin-associated proteins in motility and chemotaxis of *Dictyostelium* cells. Symp. Soc. Exp. Biol. *47*, 297–315.

Goode, B. L., Wong, J. J., Butty, A. C., Peter, M., McCormack, A. L., Yates, J. R., Drubin, D. G., and Barnes, G. (1999). Coronin promotes the rapid assembly and cross-linking of actin filaments and may link the actin and microtubule cytoskeletons in yeast. J. Cell Biol. *144*, 83–98.

Grogan, A., Reeves, E., Keep, N., Wientjes, F., Totty, N. F., Burlingame, A. L., Hsuan, J. J., and Segal, A. W. (1997). Cytosolic phox proteins interact with and regulate the assembly of coronin in neutrophils. J. Cell Sci. *110*, 3071–3081.

Guerin, I., and de Chastellier, C. (2000). Pathogenic mycobacteria disrupt the macrophage actin filament network. Infect. Immun. *68*, 2655–2662.

Heil-Chapdelaine, R. A., Tran, N. K., and Cooper, J. A. (1998). The role of *Saccharomyces cerevisiae* coronin in the actin and microtubule cytoskeletons. Curr. Biol. *8*, 1281–1284.

Humphries, C. L., Balcer, H. I., D'Agostino, J. L., Winsor, B., Drubin, D. G., Barnes, G., Andrews, B. J., and Goode, B. L. (2002). Direct regulation of Arp2/3 complex activity and function by the actin binding protein coronin. J. Cell Biol. *159*, 993–1004.

Itoh, S., Suzuki, K., Nishihata, J., Iwasa, M., Oku, T., Nakajin, S., Nauseef, W. M., and Toyoshima, S. (2002). The role of protein kinase C in the transient association of p57, a coronin family actin-binding protein, with phagosomes. Biol. Pharm. Bull. *25*, 837–844.

Jayachandran, R., Sundaramurthy, V., Combaluzier, B., Mueller, P., Korf, H., Huygen, K., Miyazaki, T., Albrecht, I., Massner, J., and Pieters, J. (2007).

Survival of mycobacteria in macrophages is mediated by coronin 1-dependent activation of calcineurin. Cell *130*, 37–50.

Johannes, L., and Lamaze, C. (2002). Clathrin-dependent or not: is it still the question? Traffic *3*, 443–451.

Maniak, M., Rauchenberger, R., Albrecht, R., Murphy, J., and Gerisch, G. (1995). Coronin involved in phagocytosis: dynamics of particle-induced relocalization visualized by a green fluorescent protein Tag. Cell *83*, 915–924.

Nal, B., Carroll, P., Mohr, E., Verthuy, C., Da Silva, M. I., Gayet, O., Guo, X. J., He, H. T., Alcover, A., and Ferrier, P. (2004). Coronin-1 expression in T lymphocytes: insights into protein function during T cell development and activation. Int. Immunol. *16*, 231–240.

Nguyen, L., Walburger, A., Houben, E., Koul, A., Muller, S., Morbitzer, M., Klebl, B., Ferrari, G., and Pieters, J. (2005). Role of protein kinase G in growth and glutamine metabolism of *Mycobacterium* bovis BCG. J. Bacteriol. *187*, 5852–5856.

Okumura, M., Kung, C., Wong, S., Rodgers, M., and Thomas, M. L. (1998). Definition of family of coronin-related proteins conserved between humans and mice: close genetic linkage between coronin-2 and CD45-associated protein. DNA Cell Biol. *17*, 779–787.

Pantaloni, D., Le Clainche, C., and Carlier, M. F. (2001). Mechanism of actin-based motility. Science *292*, 1502–1506.

Parente, J. A., Jr., Chen, X., Zhou, C., Petropoulos, A. C., and Chew, C. S. (1999). Isolation, cloning, and characterization of a new mammalian coronin family member, coroninse, which is regulated within the protein kinase C signaling pathway. J. Biol. Chem. *274*, 3017–3025.

Pieters, J. (2001). Evasion of host cell defense mechanisms by pathogenic bacteria. Curr. Opin. Immunol. *13*, 37–44.

Rybakin, V., and Clemen, C. S. (2005). Coronin proteins as multifunctional regulators of the cytoskeleton and membrane trafficking. Bioessays *27*, 625–632.

Scherr, N., Honnappa, S., Kunz, G., Mueller, P., Jayachandran, R., Winkler, F., Pieters, J., and Steinmetz, M. O. (2007). From the cover: structural basis for the specific inhibition of protein kinase G, a virulence factor of *Mycobacterium tuberculosis*. Proc. Natl. Acad. Sci. USA *104*, 12151–12156.

Schuller, S., Neefjes, J., Ottenhoff, T., Thole, J., and Young, D. (2001). Coronin is involved in uptake of *Mycobacterium* bovis BCG in human macrophages but not in phagosome maintenance. Cell Microbiol. *3*, 785–793.

Smith, T. F., Gaitatzes, C., Saxena, K., and Neer, E. J. (1999). The WD repeat: a common architecture for diverse functions. Trends Biochem. Sci. *24*, 181–185.

Steinman, R. M., and Swanson, J. (1995). The endocytic activity of dendritic cells. J. Exp. Med. *182*, 283–288.

Suzuki, K., Nishihata, J., Arai, Y., Honma, N., Yamamoto, K., Irimura, T., and Toyoshima, S. (1995). Molecular cloning of a novel actin-binding protein, p57, with a WD repeat and a leucine zipper motif. FEBS Lett. *364*, 283–288.

Tailleux, L., Neyrolles, O., Honore-Bouakline, S., Perret, E., Sanchez, F., Abastado, J. P., Lagrange, P. H., Gluckman, J. C., Rosenzwajg, M., and Herrmann, J. L. (2003). Constrained intracellular survival of *Mycobacterium tuberculosis* in human dendritic cells. J. Immunol. *170*, 1939–1948.

Tulp, A., Verwoerd, D., Dobberstein, B., Ploegh, H. L., and Pieters, J. (1994). Isolation and characterization of the intracellular MHC class II compartment. Nature *369*, 120–126.

Vieira, O. V., Botelho, R. J., and Grinstein, S. (2002). Phagosome maturation: aging gracefully. Biochem. J. *366*, 689–704.

Walburger, A., Koul, A., Ferrari, G., Nguyen, L., Prescianotto-Baschong, C., Huygen, K., Klebl, B., Thompson, C., Bacher, G., and Pieters, J. (2004). Protein kinase G from pathogenic mycobacteria promotes survival within macrophages. Science *304*, 1800–1804.

Yan, M., Collins, R. F., Grinstein, S., and Trimble, W. S. (2005). Coronin-1 function is required for phagosome formation. Mol. Biol. Cell *16*, 3077–3087.

Zheng, P. Y., and Jones, N. L. (2003). Helicobacter pylori strains expressing the vacuolating cytotoxin interrupt phagosome maturation in macrophages by recruiting and retaining TACO (coronin 1) protein. Cell Microbiol. *5*, 25–40.